



The thorium-229 low-energy isomer and the nuclear clock

Kjeld Beeks¹, Tomas Sikorsky¹, Thorsten Schumm¹, Johannes Thielking², Maxim V. Okhapkin¹ and Ekkehard Peik^{1,2}

Abstract | The ^{229}Th nucleus has an isomeric state at an energy of about 8 eV above the ground state, several orders of magnitude lower than typical nuclear excitation energies. This has inspired the development of a field of low-energy nuclear physics in which nuclear transition rates are influenced by the electron shell. The low energy makes the ^{229}Th isomer accessible to resonant laser excitation. Observed in laser-cooled trapped thorium ions or with thorium dopant ions in a transparent solid, the nuclear resonance may serve as the reference for an optical clock of very high accuracy. Precision frequency comparisons between such a nuclear clock and conventional atomic clocks will provide sensitivity to the effects of hypothetical new physics beyond the standard model. Although laser excitation of ^{229}Th remains an unsolved challenge, recent experiments have provided essential information on the transition energy and relevant nuclear properties, advancing the field.

Although we are used to speaking about atomic clocks, the origin of these devices can be traced to research on nuclear physics. In 1924, Wolfgang Pauli pointed out that some splittings of atomic spectral lines originate from the coupling between the magnetic moments of the nucleus and the electrons¹. In 1935, Hendrik Casimir showed that a line splitting of comparable magnitude but with a different spectral pattern is produced by the electric interaction when the charge distribution of the nucleus is not spherically symmetric². Based on precision measurements of this hyperfine structure, the spectroscopy of atomic transitions became an important source of information about nuclear properties. The group of Isidor Rabi investigated atomic beams interacting with microwave radiation³. Some of the resonances could be recorded with such excellent reproducibility that Rabi proposed in 1945 to use them in “the most accurate of timepieces”⁴. This was the seminal idea for the caesium atomic clock that has been the underpinning of time keeping for decades⁵. Although the fields of atomic and nuclear physics expanded in diverse directions in the second half of the twentieth century, an emerging topic is now creating new links between the two domains, with the concept of a highly precise clock once again playing a central role.

The resonance frequency of the Cs clock at about 9.2 GHz is determined by the properties of the ^{133}Cs nucleus, the valence electron and their electromagnetic interactions. In a well-designed clock, the atoms are protected from external perturbations that would otherwise shift the resonance frequency. In recent years, much progress towards greater accuracy has been made in

optical clocks⁶ that make use of resonance frequencies of transitions in the atomic electron shell in the optical frequency range ($\sim 10^{15}$ Hz). Reaching accuracies in the 10^{-18} range (comparable to missing 1 s over the age of the Universe), it is critical to control all interactions of the atom with the environment, for example the thermal radiation emitted by surfaces surrounding the atoms. The prospect of finding a reference oscillator that is less sensitive to external fields has motivated the concept of an optical nuclear clock⁷, first proposed in 2003. The small size of the nucleus and tight binding of its constituents make resonant frequencies associated with internal excitations highly insensitive to external fields^{7,8}. But the strong binding inside the nucleus also places the characteristic energies for electromagnetic transitions in the 0.1–1 MeV range, orders of magnitude above the photon energies used in current atomic clocks.

Fortunately, nature has provided a system for developing a nuclear clock in the optical frequency range: the low-energy isomer in ^{229}Th (REFS^{9–11}). The ^{229}Th nucleus is unique in nuclear physics in providing the only isomer energy in the range of the outer-shell electronic transitions. In addition to its relevance for the nuclear clock, this property also opens opportunities for experimental studies of low-energy nuclear physics, where nuclear and electronic excitations can couple because they appear in the same energy range^{12–14}. However, a main experimental challenge is to drive this nuclear excitation resonantly with a narrowband tunable laser, which would constitute a milestone in the development of the nuclear clock and is the goal of several ongoing experiments^{10,11}.

¹Vienna Center for Quantum Science and Technology, Atominstitut, TU Wien, Vienna, Austria.

²Physikalisch-Technische Bundesanstalt, Braunschweig, Germany.

✉e-mail: ekkehard.peik@ptb.de

<https://doi.org/10.1038/s42254-021-00286-6>

Key points

- A nuclear clock, based on a radiative transition in the nucleus, is less sensitive to external perturbations and therefore potentially more precise than established atomic clocks that are based on transitions in the electron shell.
- The ^{229}Th nucleus is the prime candidate for the realization of a nuclear clock because it possesses a low-energy (8 eV) excited state that is amenable to resonant laser excitation from the nuclear ground state, with an expected natural linewidth in the millihertz range.
- Recent experiments have provided essential information on the nuclear properties of ^{229}Th (half-life 7,920 years), such as the nuclear moments, decay modes of the isomer and a more precise value of the isomer excitation energy, which is required to achieve laser excitation.
- Thorium-229 is studied as trapped atomic ions in vacuum or doped into transparent crystals such as CaF_2 . Because the nuclear transition energy is in the range of transitions of valence electrons, the electronic state may influence the nuclear excitation and decay rates.
- Because of a fine balance of contributions from the strong and electromagnetic interactions to the nuclear transition energy, a ^{229}Th clock would be sensitive to predicted effects of physics beyond the standard model, such as temporal or spatial variations of fundamental constants.

In this Review, we will discuss research activities on the ^{229}Th low-energy isomer that have resulted in new experimental methods and insights into the properties of the nucleus, together with a steady stream of ideas for further research and applications. Other reviews of the field can be found in REFS^{10,11,15–17}.

Properties, production and sample preparation

Thorium-229 is a radio-isotope (FIG. 1): it has a half-life of $T_{1/2} = 7,917$ years and decays entirely through α -decay with energy $Q_\alpha = 4,845$ keV (REF.¹⁸). Owing to the short half-life, ^{229}Th is not a primordial element; it has to be actively produced in nuclear decay or fission processes. The current global stock of ^{229}Th is derived from man-made ^{233}U which amounts to about 1 metric tonne, bred in nuclear reactors during the Cold War. It is estimated that there are about 750 grams of ^{229}Th , out of which only about 40 grams have isotopic purity that is sufficient for spectroscopic experiments as discussed here^{19,20}. Production through other isotopes is being investigated, owing to renewed interest in ^{229}Th for medical applications²¹.

The spin and parity of the ^{229}Th nuclear ground state have been determined to be $I^\pi = 5/2^+$ (REFS^{22,23}). The isomeric state was assigned $I^\pi = 3/2^+$ (REF.²⁴) and experimentally verified in REF.²⁵. The magnetic dipole moment (μ , expressed in nuclear magneton μ_N) and the spectroscopic electric quadrupole moments (Q_s) are $\mu = 0.360(7)\mu_N$ and $Q_s = 3.11(6)$ eb for the ground state²⁶, and $\mu = -0.37(6)\mu_N$ and $Q_s = 1.74(6)$ eb for the isomeric state, respectively²⁵. Measurements of the isomer energy and other nuclear structure properties are described in detail in the next section.

The low-lying isomer energy emerges as the consequence of a fine interplay between the nuclear rotation-vibration degrees of freedom and their coupling to the motion of the unpaired neutron (FIG. 2). The radiative nuclear transition from the isomer to the ground state is predicted to be of mixed magnetic dipole (M1) and electric quadrupole (E2) character²⁷, resulting in a lifetime in the range of 10^4 s. If energetically possible, transfer

of the isomer excitation energy to an electron from the shell proceeds much faster than radiative decay, and an internal conversion lifetime of 7 μs has been observed for neutral Th (REF.²⁸).

Three nuclear decay processes lead into ^{229}Th : α -decay of ^{233}U , β -decay of ^{229}Ac , and electron capture decay of ^{229}Pa (FIG. 1). The α -decay of ^{233}U ($T_{1/2} = 1.6 \times 10^5$ years) is currently the only means to obtain usable quantities of ^{229}Th . An energy of $Q_\alpha = 4,824$ keV is released in the α -decay, transferring a recoil energy of 84 keV onto the ^{229}Th nucleus. This energy is sufficient to eject ^{229}Th recoil ions from thin layers (few tens of nanometres) of ^{233}U , which can be used to produce a ^{229}Th recoil ion source (see the following section). Only 2% of the ^{233}U α -decay events lead to a population of the low-energy ^{229}Th isomer^{9,25,29,30}. This method has been the most successful way to produce isomeric ^{229}Th in a series of breakthrough experiments (see next sections).

As an alternative, the β -decay of ^{229}Ac ($T_{1/2} = 62.7$ min) can be used to produce (isomeric) ^{229}Th . Actinium-229 undergoes 100% β -decay ($Q_\beta = 1.1$ MeV) to ^{229}Th . Population of the ^{229}Th isomer is more than 14%, at least a factor of 7 above the yield obtained in ^{233}U α -decay³¹. The recoil on the ^{229}Th nucleus is at most 2.3 eV (REF.³²), below typical displacement energies of solids. The production of ^{229}Ac in the ISOLDE facility at CERN has been demonstrated³³, and the use of ^{229}Ac to populate the ^{229}Th isomer and measure the isomer energy via direct radiative decay has been proposed³¹.

Thorium-229 is also obtained in the electron capture decay of ^{229}Pa ($T_{1/2} = 1.5$ days); however, production of ^{229}Pa remains a challenge in itself. Thorium-229 can also be produced in radioactive beam facilities, such as the Ion Guide Isotope Separation On-Line (IGISOL), for example in a $^{232}\text{Th}(p,p3n)^{229}\text{Th}$ light-ion-induced fusion-evaporation reaction. The cross-sections for this reaction are currently being determined.

Two types of preparation of the nuclei are predominantly used in experiments aimed towards the use of ^{229}Th for a nuclear clock: Th atomic ions in radiofrequency (RF) ion traps, and Th-doped optically transparent crystals. These systems are suitable for optical spectroscopy with a small number of nuclei of the rare isotope (to the extreme of working with a single trapped ion), and they permit researchers to study the radiative excitation and decay of the isomer without non-radiative energy transfer via the electron shell, as would be the case in neutral Th atoms or Th metal.

Ion traps. Since their introduction in 1958, RF traps have been used successfully to investigate the properties of ions isolated from environmental perturbations³⁴. Ion traps are used in some of the most accurate atomic clocks currently available, reaching fractional uncertainties of the order of 10^{-18} (REFS^{35,36}).

Several experiments have used linear RF traps to perform precision spectroscopy on Th ions in various charge states (see REFS^{37–39}). The charge states Th^+ and Th^{3+} have been used to search for interactions between the electron shell and the nucleus. Having three and two valence electrons respectively, their dense electronic level structures are likely to interact with the low-lying

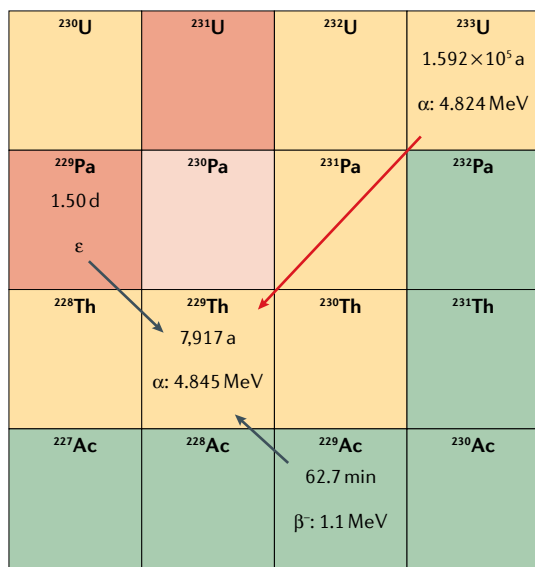


Fig. 1 | Section of the table of nuclides showing the natural decay paths leading to the production of (isomeric) ^{229}Th . The table shows α -decay (yellow) of ^{233}U , β^- -decay (green) of ^{229}Ac and electron capture ε of ^{229}Pa (red). Half-lives are given in days (d) or years (a).

nuclear transition. However, these charge states lack suitable closed electronic transitions for laser cooling. Techniques such as sympathetic laser cooling using a different ion of comparable charge-to-mass ratio⁴⁰ or buffer-gas cooling with a neutral atom or molecule³⁷ are therefore necessary. Buffer-gas cooling with a rare gas at room temperature is easy to implement, but still leads to sizeable Doppler-broadening and a loss of Th ions through reactions with impurities in the background gas. Collisions with the buffer gas are also used to depopulate metastable states, which otherwise would need to be repumped with lasers⁴¹.

The charge states Th^{3+} and Th^{4+} have been considered for the realization of the nuclear clock based on trapped ions¹⁰. The Th^{3+} ion has only one valence electron and a much lower density of electronic levels than Th^+ . This makes it easier to prepare an electronic state that minimizes the perturbation of the nuclear transition^{7,8}. Although it has been shown that $^{229}\text{Th}^{3+}$ can be directly laser cooled³⁸, sympathetic cooling with another isotope³⁸ ($^{232}\text{Th}^{3+}$) or element⁴⁰ (such as Ca^+ or Sr^+) may be more convenient as it avoids the need for optical pumping between multiple hyperfine sublevels.

Since the charge state Th^{4+} has a Rn-like closed shell of valence electrons, it is expected to be even less sensitive to external perturbations, although effects such as Sternheimer antishielding need to be considered⁴². The closed electron shell also does not offer suitable transitions for laser cooling and hyperfine spectroscopy, requiring methods such as quantum logic spectroscopy⁴³ with an auxiliary ion for cooling and readout of the nuclear state.

The two main techniques used so far to load Th ions into RF traps are recoil ions from a uranium source⁴⁴ and laser ablation from a solid Th compound such as thorium nitrate (see REFS^{37–39}). A uranium recoil source

produces Th ions in several charge states up to Th^{10+} or even higher^{45,46}. However, the extracted charge-state distribution is lowered by charge exchange when a buffer gas is used to reduce the initial kinetic energy. In the case of laser ablation, the produced charge state and number of ions strongly depend on the applied laser intensity and sample activity, with Th^{3+} being the highest charge state reached so far (see REFS^{47,48}).

Solid-state samples. In 2003, it was suggested⁷ that the favourable properties of the ^{229}Th isomer clock transition should persist even in a solid-state environment, sparking the idea of a ‘solid-state nuclear clock’ that would make use of a much higher particle number, possibly 10 or more orders of magnitude higher than in the trapped ion approach. Thorium-229 doping concentrations of $\sim 10^{17} \text{ cm}^{-3}$ (corresponding to $\sim 0.01\%$ concentration) have been realized experimentally^{49,50}.

The ^{229}Th ions would be embedded (doped) into large-bandgap crystal matrices, transparent in the vacuum-ultraviolet (VUV) range⁷. This system was investigated theoretically and experimentally for various host materials, mainly fluoride crystals such as CaF_2 , MgF_2 , Li CaAlF_6 or LiSrAlF_6 (REFS^{51–53}). These samples serve as targets for attempts to directly excite the ^{229}Th isomer using synchrotron radiation, lasers, or X-ray pumping via higher-excited nuclear states⁵⁴.

Doping ^{229}Th into a single crystal is expected to lead to a Th^{4+} charge state, where the four valence electrons of neutral Th are bound by the surrounding crystal matrix. In most cases, this charge compensation locally modifies the crystal structure, creating vacancies or interstitial ions (mostly F^-). These defects (sometimes referred to as colour centres) lead to the emergence of new electronic states within the bandgap, spatially localized at the defect position. The electron wavefunctions involved have an overlap with the ^{229}Th nucleus and can lead to additional coupling mechanisms.

Previously regarded as a nuisance, these electronic defect states have recently been discussed as a means to populate, probe or quench the isomeric state, in loose analogy to electronic bridge mechanisms in ions⁵⁵. Generally, the nuclear coupling to these defect states is weak, not significantly altering the expected spontaneous decay rate for $4+$ ions. However, electronic defect states provide an intermediate level for two-photon excitations, enabling the use of powerful lasers at longer wavelength, and an increase in the excitation rate by two orders of magnitude compared with direct radiative excitation has been conjectured for the $\text{Th}:\text{CaF}_2$ system. At present, these are theoretical considerations, as long as little information about the microscopic structure of Th doping is available. The energy and linewidth of the defect states remain to be measured experimentally for different host materials.

The interaction of nuclear moments with the crystal fields leads to the emergence of level shifts, splittings and broadenings^{56,57}. All these effects need to be considered and quantified carefully in the design and operation of a solid-state-based nuclear clock. In particular, the nuclear quadrupole interaction with electric field gradients leads to the emergence of a quadrupole

Sternheimer antishielding
An external electric field gradient may be strongly enhanced at the position of the nucleus by the influence of the deformed electron shell, especially in heavy atoms.

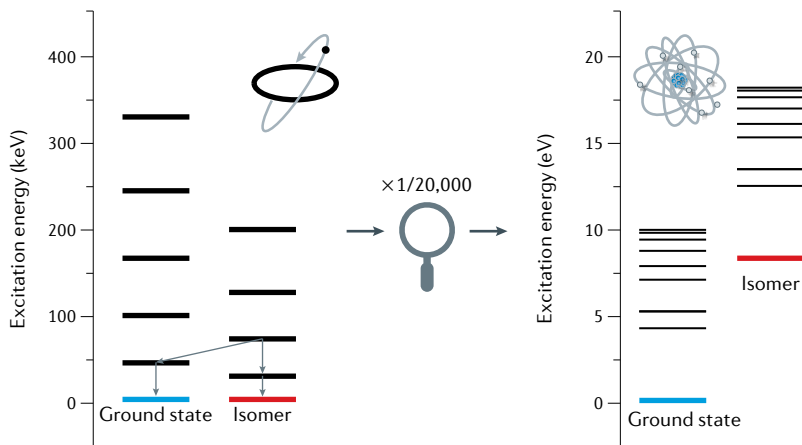


Fig. 2 | Schematic of the energy levels of ^{229}Th . The nuclear level structure (left) can be described in terms of an elliptic core and an unpaired neutron, and is structured into rotational bands. The ground state (blue) and the isomeric state (red) are the band heads (of lowest angular momentum) to two different bands, and nearly degenerate in energy by coincidence. The grey arrows indicate the cascades of γ -transitions that have been used in the first measurements of the isomer energy. On an energy scale stretched 20,000 times (right), the two lowest nuclear states together with their electronic level structure are shown. Thick lines indicate nuclear levels, thin lines electronic excited states. The electronic structure (shown here simplified) of Th^+ results from mixed configurations of the valence electrons.

hyperfine structure. The resulting level splittings are expected in the range of 50–500 MHz, depending on the local field gradient at the position of the nucleus. They can be used for non-destructive state monitoring in nuclear quadrupole resonance spectroscopy and in schemes exploiting nuclear superradiance⁵⁸. Interestingly, precision laser spectroscopy on the ^{229}Th nuclear transition in the solid state would transfer the method of Mössbauer spectroscopy into the optical regime, maintaining the benefits of a recoil-free resonance line and adding the advantages of using a coherent radiation source.

Transparent crystals are also used as implantation hosts for experiments using ^{229}Th recoil ions from external or internal ^{233}U sources (REFS^{59,60}), laser ablation plasmas⁶¹ or ion beams from isotope facilities³¹. In contrast to doping, implantation samples leave the Th ions in an uncontrolled microscopic chemical environment. In general, crystal damage caused by the intrinsic Th radioactivity and exposure to the VUV or X-ray sources generates luminescence background signal⁶², and effective suppression or filtering schemes need to be devised.

Measured isomer energy and nuclear moments

Gamma-ray measurements. The existence of the isomeric state in ^{229}Th was first deduced⁹ from γ -ray spectroscopy of ^{233}U in 1976. A consistent description of the observed γ -rays required the existence of an isomeric state, almost degenerate with the ground state. The experimental resolution of 450 eV allowed an upper bound to be placed on the isomer energy, $E_{\text{is}} < 100$ eV. In a second experiment performed in 1985, several γ -ray energies in the range from 29 keV to 320 keV of $^{233}\text{U} \rightarrow ^{229}\text{Th}$ α -decay were determined with a precision of a few electronvolts⁶³.

Mössbauer spectroscopy
High-resolution, recoil-free gamma-ray spectroscopy performed with nuclei in solids, tuned via the Doppler shift between a moving source and stationary absorber.

These were used to obtain a more precise estimate of the isomer energy to be $-1(4)$ eV (REF.⁶⁴).

An improved version of the experiment was performed in 1994 by the same group⁶⁵, and the isomer energy was determined to be $3.5(1.0)$ eV. This remained the accepted value for more than a decade, triggering a series of attempts to observe ‘nuclear fluorescence’ from α -decaying ^{233}U directly. First claims of observation^{66,67} were quickly identified as the α -decay-induced fluorescence of nitrogen^{68,69}, as these experiments were performed in air. In 2005, the experimental data from REF.⁶⁵ were re-analysed by including the effects of interband transitions, and the value of $5.5(1.0)$ eV for the isomer energy was obtained⁷⁰.

In 2007, a cryogenic microcalorimeter with 30-eV resolution was used to resolve the closely spaced transitions at 29.19 keV and 29.39 keV, as well as at 42.43 keV and 42.63 keV (REFS^{30,71}). This allowed the isomer energy to be extracted as:

$$E_{\text{is}} = (29.39 - 29.19 + 42.43 - 42.63) \text{ keV} \quad (1)$$

This method is less sensitive to the detector’s energy calibration because only the energy differences of closely spaced transitions are used. However, the authors did not report any systematic uncertainty, and it was argued that the actual uncertainty might be higher than quoted in the final result^{29,72} of $7.8(5)$ eV. In 2019, a calorimetric experiment with full-width at half-maximum FWHM = 40 eV reported the isomer energy to be $8.3(9)$ eV. This value is consistent with the previous reports, but does not decrease the uncertainty.

The 29.19-keV and 42.43-keV lines are doublets with spacings equal to the isomer energy (see FIG. 3). A recent experiment using a cryogenic microcalorimeter with 10-eV resolution succeeded in resolving the 29.19-keV doublet⁷³. The isomer energy can also be extracted directly from the splitting of the doublet lines. The isomer energy was found to be $8.10(17)$ eV using the double difference method (equation (1)) and $7.84(29)$ eV from the splitting of the 29.19-keV doublet. From the lineshape of the 29.19-keV doublet, the improved value of the branching ratio, b_{29} , was measured to be $b\left(\frac{29.19 \text{ keV} \rightarrow 8 \text{ eV}}{29.19 \text{ keV} \rightarrow 0 \text{ eV}}\right) = b_{29} = 9.3(6)\%$.

Internal conversion measurements. The first direct signature of the ^{229}Th isomer was obtained in 2016, about 30 years after first being predicted⁷⁴. In this experiment, rather than the radiative decay of the isomer, internal conversion (IC) was detected. IC is a process in which the nuclear excitation energy is transferred to the electron shell, causing the ejection of a valence electron, which can then be detected⁷⁵.

The set-up in REF.⁷⁴ consisted of three parts: production cell, filter and detector. The production cell used a ^{233}U recoil source and a buffer-gas stopping cell to slow down the energetic radioactive decay products and guide them towards an exit nozzle. All ^{233}U decay products are in an ionized state and can be filtered by a quadrupole mass spectrometer selecting for ^{229}Th , of which 2% is in the isomeric state. This filtered ion beam was directed to a microchannel plate (MCP), where the

impacting ion created a ‘prompt’ signal. Successively, the ion neutralizes by attracting electrons from the MCP metallized surface. Although energetically forbidden for the ion, in the neutral ^{229}Th the excited nucleus can rapidly transfer its energy to a valence electron (IC), which creates a second signal on the detector, delayed by several microseconds²⁸.

To measure the energy of the ^{229}Th isomer, a magnetic bottle-type retarding field spectrometer⁷⁶ was added. The ions are guided through a graphene foil, which neutralizes them in-flight and triggers the IC process. The emitted electrons are magnetically guided towards a second MCP. A retardation voltage is used to measure the kinetic energy of the electrons. By combining the measured kinetic energy of the electrons with the remaining internal energy of Th, the isomer energy can be determined to be 8.28(17) eV. The uncertainty in this energy predominantly arises from unresolved distributions of initial and final electronic configurations of the ^{229}Th atom/ion in this process. The consistency of this result with the recent γ -measurements provides the desired confidence for building a dedicated VUV laser system for a nuclear clock in this wavelength region.

The success of using the IC process as a detection channel for the ^{229}Th isomer inspired a new experiment that is currently being prepared at the University of California, Los Angeles and JILA. The concept is to combine narrowband laser excitation with IC detection. In a recent proposal, it was shown that this combination could determine the nuclear clock transition frequency to 100-MHz precision using a VUV frequency comb⁷⁷. Efforts are also underway to use a superconducting nanowire single-photon detector to replace the MCP and the magnetic bottle spectrometer to determine the isomer energy more accurately⁷⁸.

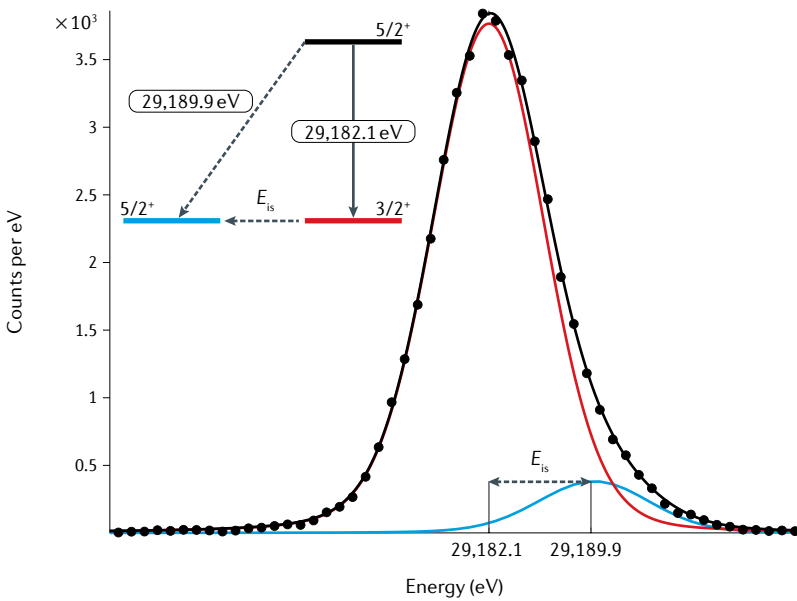


Fig. 3 | Lineshape of the 29.19-keV doublet. The red curve represents the fit of the intraband $5/2^+ \rightarrow 3/2^+$ transition, and the blue curve represents the fit of the interband $5/2^+ \rightarrow 5/2^+$ transition. The black line is the sum of both transitions reprinted with permission from REF.⁷³, APS. Both the branching ratio and the isomer energy can be extracted directly from this fit. Inset, nuclear energy level diagram. The raw data are available in the Zenodo repository¹²¹.

Nuclear moments of the isomer. Owing to the interaction between the nucleus and the electron shell, several nuclear parameters can be determined by performing precision spectroscopy on atomic transitions. The magnetic dipole moment μ and the electric quadrupole moment Q can be determined from the hyperfine splitting of electronic levels. A change of the mean squared charge radius r^2 between different isotopes and isomers can be measured from the relative isotope shift of these levels⁷⁹.

The magnetic dipole moment of the nuclear ground state of ^{229}Th has been measured in several experiments based on hyperfine spectroscopy^{22,26,79}. The most precise value of $\mu = 0.360(7) \mu_N$ was obtained by precision spectroscopy of laser-cooled $^{229}\text{Th}^{3+}$ ions, combined with state-of-the-art atomic theory to calculate the electron wavefunction²⁶. The same experiment also provided a measurement of the electric quadrupole moment $Q = 3.11(6)$ eb, which agrees with an earlier value of $Q = 3.149(32)$ eb obtained via Coulomb excitation⁸⁰.

Experimental values $\mu = -0.37(6) \mu_N$ and $Q = 1.74(6)$ eb for the nuclear moments of the isomeric state were first obtained in 2018 by comparing the hyperfine structure of two electronic transitions in $^{229}\text{Th}^{2+}$ ions in ground (^{229}gTh) and isomeric ($^{229\text{m}}\text{Th}$) states, which were produced by a ^{233}U recoil source²⁵. These values confirmed predictions for the quadrupole moment⁸¹ and agree with current nuclear model calculations for the magnetic dipole moment^{82,83}. The experiment in REF.²⁵ also determined the change in mean squared charge radius between ^{229}gTh and $^{229\text{m}}\text{Th}$ as $\langle r_{229\text{m}}^2 \rangle - \langle r_{229\text{g}}^2 \rangle = 0.012(2) \text{ fm}^2$ by comparing the isomeric shift of selected electronic transitions with their respective isotope shift between ^{232}Th and ^{229}Th . The result shows quantitatively that in the excitation to the isomeric state, not only an unpaired neutron, but also the proton distribution of ^{229}Th is affected.

By using the parameters μ , Q and r^2 of both nuclear states, the hyperfine structure of an electronic transition of the isomer can be predicted when the structure is known for the nuclear ground state (see FIG. 4 for a selected transition of Th^{3+}). This enables a highly efficient, non-demolition detection scheme for the isomeric state based on hyperfine spectroscopy, known as double resonance^{7,84,85}.

Methods for exciting the ^{229}Th isomer

So far, all of the successful experiments described above used the α -decay of ^{233}U as a means to generate ^{229}Th in the isomeric state. Although conceptually simple and reliable, this mechanism only has a 2% efficiency. Furthermore, it transfers 84 keV recoil energy to the freshly born ^{229}Th ion, often leaving it in an uncontrolled state concerning kinetics and charge. More efficient and controlled methods of obtaining isomeric ^{229}Th are hence under investigation. These approaches can be coarsely divided into two main groups: one that exploits various coupling mechanisms between the electronic level structure and the nuclear ground and isomeric state, and one that uses light-induced transitions within the nuclear level structure only (FIG. 5). Both are briefly discussed in the following.

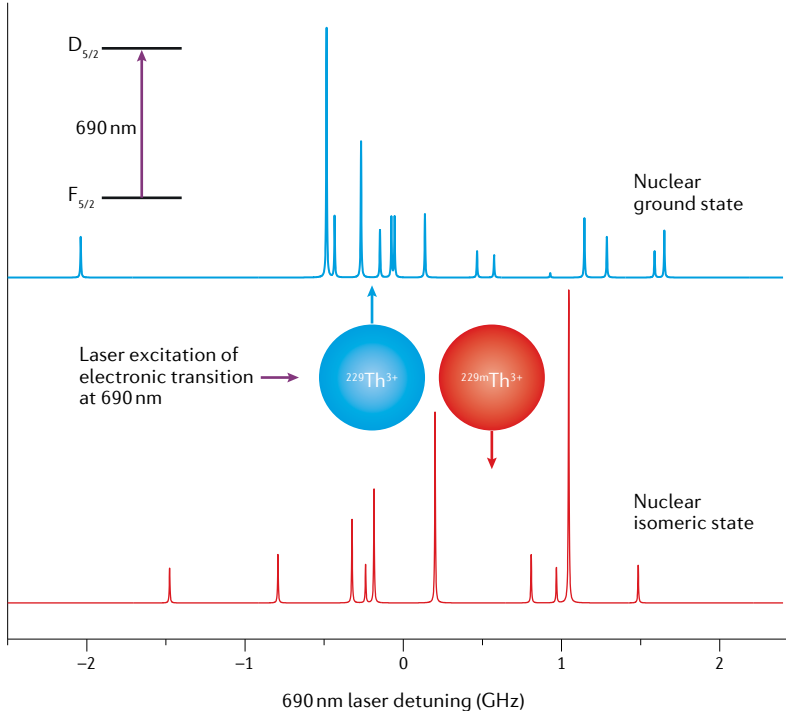


Fig. 4 | Simulated hyperfine structure of the $F_{5/2} \rightarrow D_{5/2}$ electronic transition at 690 nm in $^{229}\text{Th}^{3+}$ for the nuclear ground state and the isomer. Blue trace, nuclear ground state; red, isomer. The amplitudes are calculated assuming a uniform population of initial hyperfine states. The structures differ owing to the difference in spin, nuclear moments and mean squared charge radius between the two nuclear states^{25,26}. This can be used to distinguish the two nuclear states via hyperfine spectroscopy.

Nuclear excitation via electronic resonance. The ^{229m}Th isomer has the unique property that its excitation energy is of the same order as processes of the outer-shell electrons. Interactions with the electron shell can, therefore, be expected to enhance the nuclear excitation and de-excitation rates significantly^{86,87}. This can be exploited to achieve the excitation of the nucleus in a multiphoton process via nuclear excitation by electron transition (NEET) or the electronic bridge (EB) process^{88,89}.

The first attempt to excite a low-lying isomer by the NEET process was reported⁹⁰ using a laser-produced plasma of ^{235}U in 1979. A similar technique was proposed to obtain a large number of ^{229}Th isomeric nuclei⁹¹, and a corresponding experimental attempt was performed⁶¹ in 2018. Although the results of this work were not reported in a peer-reviewed journal, the excitation of the Th isomer in a laser-produced plasma merits further investigation.

In the case of ionized thorium, the nuclear excitation energy lies below the ionization potential⁹². NEET/EB excitation schemes are therefore concentrated on transitions between bound electronic states. In a scheme proposed for Th^+ ions, the electron shell is excited by two photons whose sum of frequencies equals the nuclear transition frequency, thereby coupling to the isomeric state⁹³.

Alternatively, it has been proposed to resonantly populate higher-lying electronic states in order to excite the nucleus in a two-photon decay process (see, for example, REF.⁹⁴). Corresponding experiments are

currently performed with trapped Th^+ and Th^{2+} ions, which are characterized by their comparably high electronic level density in the energy range of the isomer^{39,95,96}.

Excitation via the EB process has also been proposed for highly charged Th^{3+} ions in electron-beam ion traps⁹⁷. With increasing charge, fine-structure splittings in the electronic ground-state configuration become larger and eventually reach the value of the nuclear transition energy, at about the Th^{3+} charge state. Since several fine-structure transitions with the same multipolarity as the nuclear transition are available, a highly efficient EB coupling can be expected.

In the case of the decay of the isomeric state, the laser-induced electronic bridge (LIEB) process can be used to achieve precise knowledge of the nuclear excitation energy⁹⁸. In this scheme, a Th ion in the isomeric state is excited to a virtual electronic state. If this state is in resonance with an electronic excitation of the nuclear ground state, the nuclear decay is strongly enhanced. The nuclear excitation energy can then be inferred from the photon energy and the addressed electronic level.

Direct excitation of nuclear levels by synchrotron radiation. A series of attempts were made to resonantly excite the ^{229}Th nucleus from the ground state to excited nuclear states by using synchrotron or undulator sources of VUV light, and to detect the ensuing fluorescence decay or other signals indicating successful excitation.

The first set of investigations focused on direct radiative excitation of the isomeric state. In 2014/15, ^{229}Th -doped LiSrAlF_6 crystals (10^{16} – 10^{17} cm $^{-3}$ concentration) were used at the Advanced Light Source (ALS) synchrotron to optically excite the isomer⁴⁹. ALS provided a 0.19-eV-linewidth source with an integrated flux of $\sim 7 \times 10^{14}$ photons s $^{-1}$, tunable between 7.3 eV and 8.8 eV. A spectroscopic search for the nuclear resonance was performed during a 96-h run, scanning the interval in 0.1-eV steps with 2,000 s illumination time. No nuclear fluorescence signal could be detected, which allowed the exclusion (90% confidence level) of short isomer lifetimes (between 1 s and 2,000 s) in the scanned energy interval, assuming that non-radiative decay processes are negligible in the crystal.

A conceptually identical experiment was performed in 2017 at the Metrology Light Source (MLS) synchrotron⁶². This time, a ^{229}Th -doped CaF_2 crystal (10^{16} cm $^{-3}$ concentration) was used to scan for the isomer in the energy region 7.5–10 eV, again without success. A sample of surface-absorbed ^{229}Th nitrate on a CaF_2 carrier substrate has also been investigated at MLS in the energy range 3.9–9.5 eV (REF.⁹⁹). Again, no nuclear fluorescence signal could be detected.

These experiments highlight the need for a detailed understanding of the microscopic electronic structure and the relevance of non-radiative decay processes in solid-state samples.

A different approach consists of X-ray pumping via higher-excited nuclear states, using narrowband synchrotron radiation. A pumping rate of 25 kHz into the isomeric state was demonstrated in an experiment

carried out at the SPring-8 synchrotron source, actively exciting ^{229}Th from the ground state into the 29-keV second excited state⁵⁴.

Resonant laser excitation. Towards the demonstration of a nuclear clock, the challenge remains to drive the nuclear excitation directly and resonantly with a narrow-band laser. Direct laser excitation of the ^{229}Th isomer is a complex task owing to the current significant uncertainty in the nuclear transition energy, and challenges in the development of the laser radiation sources and operation in the VUV range. The development of dedicated laser systems for ^{229}Th nuclear spectroscopy is required and is underway in several groups worldwide.

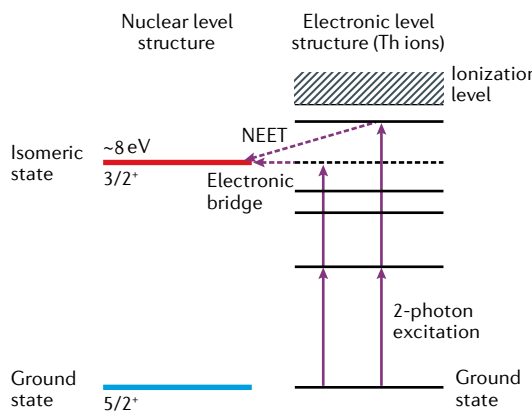
Unfortunately, nonlinear optical crystals (NLO) for the generation of the VUV light in the wavelength range of the Th isomer energy are still scarce, owing to the strong absorption of the crystals in this wavelength region¹⁰⁰. Currently, VUV light in the range of 150–156 nm has been obtained only in an optically contacted, prism-coupled $\text{KBe}_2\text{BO}_3\text{F}_2$ crystal (KBBF) by sum-frequency mixing of fundamental radiation and its fourth harmonic from pulsed Ti:sapphire laser systems^{101,102}. The VUV output power achieved in the experiments with KBBF is much lower¹⁰¹ than that for four-wave mixing based on third-order nonlinear interactions in a gas-phase medium¹⁰³.

Sum- and difference-frequency conversion of pulsed laser radiation generates coherent tunable radiation in the VUV at wavelengths 60–200 nm (REF. ¹⁰⁴). A light source using resonance-enhanced four-wave difference mixing in xenon gas (FIG. 6a) delivers high-intensity pulses of VUV light with a continuously tunable wavelength from 122 nm (10.2 eV) to 168 nm (7.4 eV)¹⁰⁵. The VUV radiation intensity of the source is in the range of 10^{13} photons per 5-ns pulse for the wavelengths 150–160 nm. The linewidth of the VUV radiation and the pulse

repetition rate of these sources are usually determined by pulsed amplifiers and lie in the range of hundreds of megahertz and tens of hertz, respectively. Typical photon spectral densities of VUV radiation at 150 nm obtained in the four-wave mixing experiments are $\sim 10^6$ photons $\text{s}^{-1} \text{Hz}^{-1}$, which corresponds to a spectral power density of $\sim 1 \text{ pW s}^{-1} \text{Hz}^{-1}$. Because of the high spectral brightness, these VUV light sources are a useful tool for the VUV spectroscopy of Th.

Demonstrations of the generation of phase-coherent frequency combs in the VUV spectral region^{106,107} open new frontiers of precision metrology¹⁰⁸ and development of optical clocks based on the nuclear transition in Th. The excitation energy of the isomeric state corresponds to the seventh harmonic generation of a cavity-enhanced Yb-fibre frequency comb¹⁰⁹ or to the fifth harmonic of a frequency comb based on a Ti:sapphire laser (FIG. 6b). Thin films as generation media for VUV light have attracted attention because they require lower laser peak intensities than gases. Intense fifth harmonic generation of a Ti:sapphire laser was demonstrated from a thin AlN crystalline film grown on a sapphire substrate¹¹⁰. Typical continuous-wave (CW) power of an individual VUV comb mode lies in the nanowatt range, depending on the laser source, the enhancement cavity and the nonlinear medium. The linewidth of the individual mode depends on the phase and amplitude noise suppression of the laser source and varies for different comb systems. The linewidths of the individual VUV modes generated by Yb-fibre combs were estimated in a few experiments to be in the range of 10 MHz (REFS ^{111,112}). Assuming a higher suppression of the laser phase noise and especially for the fifth harmonic of a Ti:sapphire optical comb, the linewidth of the individual comb mode in the range of 1 kHz might be within reach. Therefore, a spectral brightness of $\sim 10^7$ photons $\text{s}^{-1} \text{Hz}^{-1}$ might be obtained with VUV optical combs in the range of the Th isomer

a Nucleus-ion couplings



b Nucleus-solid-state couplings

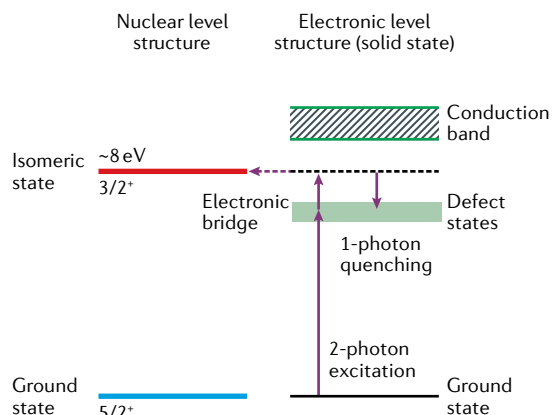


Fig. 5 | Routes to excitation of the nucleus via coupling to the electronic structure. **a** | Excitation schemes involving the ^{229}Th electronic level structure, shown here for ions in an ion trap or a plasma. The isomer can, for example, be excited in a two-photon process by a resonant electronic bridge process, or via spontaneous emission from an excited electronic state (NEET). The dashed blue arrows indicate energy transfer between the electronic and the nuclear states. **b** | Excitation and quenching schemes involving localized defect states emerging with Th dopant ions in a solid-state system. The isomer can be excited in a two-photon resonant electronic bridge process. Note that the intermediate defect state level (green band) is expected to be broad compared with electronic levels in free ions. A nuclear excitation can be quenched by shining in a single photon bridging between the nuclear and solid-state level.

energy, which is similar to four-wave mixing sources. Currently, until technology can offer suitable NLO crystals for VUV generation from CW lasers, we consider VUV optical frequency combs as the most promising light source for nuclear optical clock operation.

Assuming that the spectral power density of the VUV source is in the order of $10^6\text{--}10^7\text{ photons s}^{-1}\text{ Hz}^{-1}$ and the beam waist is $100\text{ }\mu\text{m}$, the excitation rate of the Th isomeric state can be estimated (see, for instance, REFS^{113,114}) to be about $10^{-6}\text{--}10^{-5}\text{ s}^{-1}$ for an ion in an RF trap. For ^{229}Th ions doped into a solid, we expect the nuclear transition to be broadened⁵² to a linewidth of several kilohertz. This may increase the excitation yield due to increasing spectral overlap with the excitation source, but will ultimately degrade clock performance, once probed with a hertz-level laser system.

Nuclear clock performance and applications

For applications in metrology, an important aspect of the ^{229}Th nuclear clock is the higher accuracy and robustness that it promises in comparison with optical clocks based on electronic transitions. In general, nuclear transition frequencies are less sensitive to external perturbations than transition frequencies in the electron shell because the nucleons are much more tightly bound, so that nuclear dimensions and nuclear moments are smaller. This advantage is especially important in the interaction with external electric fields. The smallness of the nuclear electric polarizability reduces frequency-shifting effects of collisions with the background gas and the interaction with the thermal radiation emitted by all surfaces surrounding the atoms. If electronic and nuclear degrees of freedom could be decoupled, the nuclear transition frequency would be independent of interactions that

produce shifts of the electronic levels. Although this is not achievable for all orders of the hyperfine interaction, it is possible to select a suitable electronic environment of the nucleus that minimizes the coupling to external perturbations. The choice may be made between electronic ground or metastable states of Th ions in various positive charge states, including Th^{3+} (favourable for trapped ion experiments), Th^{4+} (the dominant charge state of Th ions in solids) and also highly charged Th ions⁹⁷.

Two types of configurations have been identified in which the hyperfine coupled nuclear transition frequency is immune to field-induced frequency shifts to a level that cannot be obtained for an electronic transition: first, states with values 0 or $\frac{1}{2}$ of electronic or total angular momenta J or F eliminate higher-order and tensorial interactions⁷; second, stretched states with aligned orientation of the electronic and nuclear angular momenta and maximum values of F and $|m_F|$ can be obtained for all values of J and are eigenstates in the coupled as well as in the uncoupled basis⁸. For the stretched states of the $^{229}\text{Th}^{3+}$ ground state, it has been calculated that the relative frequency shift induced by thermal radiation at 300 K amounts to 1×10^{-22} , four to eight orders of magnitude smaller than in established atomic clocks⁸.

At this level of suppression of the field-induced frequency shifts, the dominant contributions to the uncertainty of a nuclear clock will be the relativistic Doppler shift from the motion of the nucleus, in the range of 10^{-18} or below for laser-cooled ions, an effect that is common to all clocks, atomic and nuclear.

In the solid-state nuclear clock, the electronic degrees of freedom are more difficult to control, and interactions with crystal fields cannot be completely avoided. In particular, the isomer shift will degrade

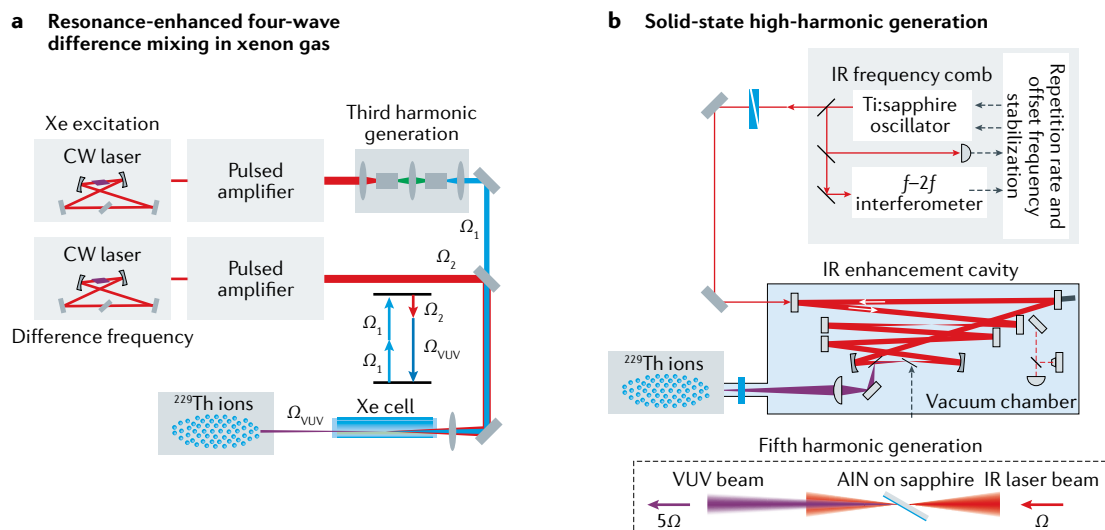


Fig. 6 | Schematics of VUV laser sources for resonant excitation of the ^{229}Th nucleus. **a |** Vacuum ultraviolet (VUV) light is generated via four-wave-difference mixing by focusing laser radiation with frequencies Ω_1 and Ω_2 into a xenon gas cell. High-intensity pulses at Ω_1 and Ω_2 are produced by seeding two pulsed amplifiers with two continuous-wave (CW) lasers and subsequent frequency tripling (in the case of Ω_1). The system can be used for interrogating the nuclear resonance of ^{229}Th ions in an ion trap or doped into a transparent host crystal. **b |** Generation of 160-nm light as the fifth harmonic of an infrared (IR) 800-nm Ti:sapphire femtosecond frequency comb. The f-2f interferometer is used to stabilize the optical phase between successive pulses. An additional photodiode stabilizes the pulse repetition rate (dashed grey lines). The harmonic generation takes place in a secondary passive enhancement cavity and uses a thin ($30\text{-}\mu\text{m}$) AlN layer as a target.

Lamb–Dicke regime
When the motion of an absorber or emitter is constrained to a region that is smaller than the wavelength, the spectrum contains a resonance that is free from the first-order Doppler shift.

the clock accuracy. On the upside, working with solid-state samples allows the interrogation of up to 10^{15} nuclei deep in the Lamb–Dicke regime, which increases the clock precision. Performances of up to 10^{-19} relative clock stability have been conjectured, but numerous questions on the interplay of the nuclear level structure with the microscopic crystal environment remain to be clarified^{56,57}.

A unique feature of the nuclear clock is its high sensitivity to possible phenomena of new physics beyond the standard model. Effects that would potentially be observable with nuclear clocks are violations of Lorentz invariance, temporal variations of fundamental constants, or coupling to additional fields such as dark matter. Such experiments have already been performed and have not detected any deviations from the standard model at the limits of precision of the best atomic clocks. A nuclear clock with higher sensitivity promises to advance the field¹⁵.

The question of the sensitivity of the ^{229}Th nuclear clock to effects of new physics has stimulated interest in the underlying nuclear structure. Even without a detailed picture of the properties of the two nearly degenerate nuclear levels that are connected by the clock transition, some insight can be gained from intuitive considerations. In contrast to a transition in the electron shell, the nuclear transition energy is not purely electromagnetic, but contains a contribution from the strong interaction. From the measured difference in the mean squared charge radius between isomer and ground state²⁵ a difference of Coulomb energy ΔE_{C} of about 100 keV between the two nuclear states can be inferred¹¹⁶. Given the small transition energy of 8 eV, it becomes clear that this change in Coulomb energy must be accompanied by a nearly equal, but opposite, change in the strong interaction energy. Because of this delicate balance, a hypothetical change in the value of the fine-structure constant α would become apparent as a change in the transition frequency $\Delta f/f = (\Delta E_{\text{C}}/E_{\text{is}})\Delta\alpha/\alpha$ that is enhanced by about four orders of magnitude⁸⁵. A similar reasoning can be applied to estimate the sensitivity to a change of the strong coupling constant^{117,118} where variations conceivably could be stronger than for α .

Even though the effects of the two interactions appear intertwined and the value of the $\Delta\alpha$ -sensitivity cannot yet be predicted precisely, the nuclear clock promises to be a highly sensitive indicator for variations of fundamental constants. The connection has been made that massive fields, such as dark matter, can produce an evolution of fundamental coupling constants of nature¹¹⁹ and, again, the ^{229}Th nuclear clock could be the suitable detector.

Violations of Lorentz invariance for massive particles would appear as an orientation dependence of the clock frequency where the sensitivity is determined by the anisotropy of the momentum distribution in the quantum states that determine the frequency. The most sensitive experiment for electrons was a comparison of two Yb^+ single-ion clocks³⁵. A similar experiment with ^{229}Th nuclear clocks would enable a test with neutrons at high sensitivity¹²⁰.

Conclusion

Burdened by the complexity of a VUV laser system as the oscillator, the ^{229}Th nuclear clock is unlikely to find applications in the mundane domains of frequency metrology such as telecommunications or navigation, at least in the short term. Moreover, since 2003 when the ^{229}Th nuclear clock was first proposed, the accuracy of optical atomic clocks has improved by more than three orders of magnitude. Notwithstanding the experimental difficulties and the strong competition from optical clocks, the prospects of the nuclear clock look as attractive as ever for opening a new field of research between atomic and nuclear physics and for new opportunities for testing fundamental physics. Recent advances in experimental methods for the preparation of ^{229}Th in different states, such as trapped ions or in solids, and the precision data now available on its nuclear properties will aid experimental progress and stimulate further conceptual ideas.

Data availability

The raw data for FIG. 3 are available in the Zenodo repository¹²¹.

Published online: 25 February 2021

- Pauli, W. Zur Frage der theoretischen Deutung der Satelliten einiger Spektrallinien und ihrer Beeinflussung durch magnetische Felder. *Naturwissenschaften* **12**, 741–743 (1924).
- Casimir, H. Über die hyperfeinstruktur des Europiums. *Physica* **2**, 719–723 (1935).
- Rabi, I. I., Zacharias, J. R., Millman, S. & Kusch, P. A new method of measuring nuclear magnetic moment. *Phys. Rev.* **53**, 318 (1938).
- Laurence, W. L. Cosmic pendulum for clock planned. *New York Times*, 34 (21 January 1945).
- Ramsey, N. F. History of early atomic clocks. *Metrologia* **42**, 1–3 (2005).
- Ludlow, A. D., Boyd, M. M., Ye, J., Peik, E. & Schmidt, P. O. Optical atomic clocks. *Rev. Mod. Phys.* **87**, 637 (2015).
- Peik, E. & Tamm, C. Nuclear laser spectroscopy of the 3.5 eV transition in Th-229. *Europhys. Lett.* **61**, 181–186 (2003). **Proposal of a high-precision optical nuclear clock based on ^{229}Th .**
- Campbell, C. J. et al. Single-ion nuclear clock for metrology at the 19th decimal place. *Phys. Rev. Lett.* **108**, 120802 (2012). **A detailed theoretical analysis of the achievable accuracy of a ^{229}Th nuclear clock with trapped ions.**
- Kroger, L. A. & Reich, C. W. Features of the low-energy level scheme of ^{229}Th as observed in the α -decay of ^{235}U . *Nucl. Phys. A* **259**, 29–60 (1976).
- Peik, E. & Okhapkin, M. Nuclear clocks based on resonant excitation of γ -transitions. *C. R. Phys.* **16**, 516–523 (2015).
- Thirolf, P. G., Seiferle, B. & von der Wense, L. The ^{229}Th isomer: doorway to the road from the atomic clock to the nuclear clock. *J. Phys. B* **52**, 203001 (2019).
- Matinyan, S. Lasers as a bridge between atomic and nuclear physics. *Phys. Rep.* **298**, 199–249 (1998).
- Tkalya, E. V. Properties of the optical transition in the ^{229}Th nucleus. *Phys. Uspekhi* **46**, 315–320 (2003).
- Pálffy, A. Nuclear effects in atomic transitions. *Contemp. Phys.* **51**, 471 (2010).
- von der Wense, L., Seiferle, B. & Thirolf, P. G. Towards a ^{229}Th -based nuclear clock. *Meas. Tech.* **60**, 13–22 (2018).
- Peik, E., Zimmermann, K., Okhapkin, M. & Tamm, C. H. R. Prospects for a nuclear optical frequency standard based on thorium-229. In *Proc. 7th Symposium on Frequency Standards and Metrology, ISFSM 2008*, 532–538 (World Scientific, 2009).
- von der Wense, L. & Seiferle, B. The ^{229}Th isomer: prospects for a nuclear optical clock. *Eur. Phys. J. A* **56**, 277 (2020).
- Varga, Z., Nicholl, A. & Mayer, K. Determination of the ^{229}Th half-life. *Phys. Rev. C* **89**, 1–6 (2014).
- Orth, D. A. SRP thorium processing experience. <https://www.osti.gov/biblio/6570656> (2020).
- Forsberg, C. W. & Lewis, L. C. Uses for uranium-233: what should be kept for future needs? *ORNL* **6952**, 7 (1999).
- Hogle, S. et al. Reactor production of thorium-229. *Appl. Radiat. Isot.* **114**, 19–27 (2016).
- Egorov, V. N. Hyperfine structure of the atomic spectrum and the nuclear moments of the thorium-229 isotope. *Opt. Spectrosc.* **16**, 549–554 (1964).
- Gulda, K., et al. The nuclear structure of ^{229}Th . *Nucl. Phys. A* **703**, 45–69 (2002).
- Litvinova, E., Feldmeier, H., Dobaczewski, J. & Flambaum, V. Nuclear structure of lowest ^{229}Th states and time-dependent fundamental constants. *Phys. Rev. C* **79**, 064303 (2009).
- Thielking, J. et al. Laser spectroscopic characterization of the nuclear-clock isomer ^{229m}Th . *Nature* **556**, 321 (2018). **Laser spectroscopic investigation of properties of the ^{229}Th isomer.**

26. Safronova, M. S., Safronova, U. I., Radnaev, A. G., Campbell, C. J. & Kuzmich, A. Magnetic dipole and electric quadrupole moments of the ^{229}Th nucleus. *Phys. Rev. A* **88**, 060501 (2013).
27. Minkov, N. & Pálffy, A. Reduced transition probabilities for the gamma decay of the 7.8-eV isomer in ^{229}Th . *Phys. Rev. Lett.* **118**, 212501 (2017).
28. Seiferle, B., von der Wense, L. & Thirolf, P. G. Lifetime measurement of the ^{229}Th nuclear isomer. *Phys. Rev. Lett.* **118**, 042501 (2017).
29. Sakharov, S. L. On the energy of the 3.5-eV level in ^{229}Th . *Phys. At. Nucl.* **73**, 1–8 (2010).
30. Beck, B. R. et al. Energy splitting of the ground-state doublet in the nucleus ^{229}Th . *Phys. Rev. Lett.* **98**, 142501 (2007). **Precise γ -spectroscopy measurement of the isomer energy.**
31. Verlinde, M. et al. Alternative approach to populate and study the ^{229}Th nuclear clock isomer. *Phys. Rev. C* **100**, 24315 (2019).
32. Kofoed-Hansen, O. On the theory of the recoil in β -decay. *Phys. Rev.* **74**, 1785–1788 (1948).
33. Ferrer, R. et al. Towards high-resolution laser ionization spectroscopy of the heaviest elements in supersonic gas jet expansion. *Nat. Commun.* **8**, 14520 (2017).
34. Paul, W. Electromagnetic traps for charged and neutral particles. *Rev. Mod. Phys.* **62**, 531 (1990).
35. Sanner, C. et al. Optical clock comparison for Lorentz symmetry testing. *Nature* **567**, 204–208 (2019).
36. Brewer, S. M. et al. ^{27}Al quantum-logic clock with a systematic uncertainty below 10^{-18} . *Phys. Rev. Lett.* **123**, 033201 (2019).
37. Kälber, W. et al. Nuclear radii of thorium isotopes from laser spectroscopy of stored ions. *Z. Phys. A* **334**, 103–108 (1989).
38. Campbell, C. J., Radnaev, A. G. & Kuzmich, A. Wigner crystals of ^{229}Th for optical excitation of the nuclear isomer. *Phys. Rev. Lett.* **106**, 223001 (2011).
39. Meier, D.-M. et al. Electronic level structure of Th^+ in the range of the ^{229}Th isomer energy. *Phys. Rev. A* **99**, 52514 (2019).
40. Groot-Berning, K. et al. Trapping and sympathetic cooling of single thorium ions for spectroscopy. *Phys. Rev. A* **99**, 023420 (2019).
41. Herrera-Sancho, O. A. et al. Two-photon laser excitation of trapped $^{232}\text{Th}^+$ ions via the 402-nm resonance line. *Phys. Rev. A* **85**, 033402 (2012).
42. Feiok, F. D. & Johnson, W. R. Atomic susceptibilities and shielding factors. *Phys. Rev.* **187**, 59–50 (1969).
43. Schmidt, P. O. et al. Spectroscopy using quantum logic. *Science* **309**, 749–752 (2005).
44. v.d. Wense, L., Seiferle, B., Laatiaoui, M. & Thirolf, P. G. Determination of the extraction efficiency for ^{233}U source α -recoil ions from the MLL buffer-gas stopping cell. *Eur. Phys. J. A* **51**, 29 (2015).
45. Haas, R. et al. Development of a recoil ion source providing slow Th ions including $^{229}\text{m}\text{Th}$ in a broad charge state distribution. *Hyperfine Interact.* **241**, 25 (2020).
46. Gunter, K., Asaro, F. & Helmholz, A. C. Charge and energy distributions of recoils from Th^{226} alpha decay. *Phys. Rev. Lett.* **16**, 362–364 (1966).
47. Zimmermann, K., Okhaphin, M. V., Herrera-Sancho, O. A. & Peik, E. Laser ablation loading of a radiofrequency ion trap. *Appl. Phys. B Lasers Opt.* **107**, 883–889 (2012).
48. Campbell, C. J. et al. Multiply charged thorium crystals for nuclear laser spectroscopy. *Phys. Rev. Lett.* **102**, 235004 (2009).
49. Jeet, J. et al. Results of a direct search using synchrotron radiation for the low-energy ^{229}Th nuclear isomeric transition. *Phys. Rev. Lett.* **114**, 253001 (2015).
50. Stellmer, S. et al. Attempt to optically excite the nuclear isomer in ^{229}Th . *Phys. Rev. A* **97**, 062506 (2018).
51. Jackson, R. A., Amaral, J. B., Valerio, M. E. G., Demille, D. P. & Hudson, E. R. Computer modelling of thorium doping in LiCaAlF_6 and LiSrAlF_6 : application to the development of solid state optical frequency devices. *J. Phys. Condens. Matter* **21**, 352403 (2009).
52. Dessoovic, P. et al. ^{229}Th -doped calcium fluoride for nuclear laser spectroscopy. *J. Phys. Condens. Matter* **26**, 105402 (2014).
53. Pimon, M. et al. DFT calculation of ^{229}Th -doped magnesium fluoride for nuclear laser spectroscopy. *J. Phys. Condens. Matter* **32**, 255503 (2020).
54. Masuda, T. et al. X-ray pumping of the ^{229}Th nuclear clock isomer. *Nature* **573**, 238–242 (2019).
55. Nickerson, B. S. et al. Nuclear excitation of the ^{229}Th isomer via defect states in doped crystals. *Phys. Rev. Lett.* **125**, 032501 (2020).
56. Rellergerdt, W. G. et al. Constraining the evolution of the fundamental constants with a solid-state optical frequency reference based on the ^{229}Th nucleus. *Phys. Rev. Lett.* **104**, 200802 (2010).
57. Kazakov, G. A. et al. Performance of a ^{229}Th solid-state nuclear clock. *N. J. Phys.* **14**, 083019 (2012).
58. Nickerson, B. S., Liao, W.-T. & Pálffy, A. Collective effects in ^{229}Th -doped crystals. *Phys. Rev. A* **98**, 062520 (2018).
59. Zhao, X. et al. Observation of the deexcitation of the ^{229}Th nuclear isomer. *Phys. Rev. Lett.* **109**, 160801 (2012).
60. Stellmer, S., Schreitl, M., Kazakov, G. A., Sterba, J. H. & Schumm, T. Feasibility study of measuring the ^{229}Th nuclear isomer transition with ^{235}U -doped crystals. *Phys. Rev. C* **94**, 14302 (2016).
61. Borisjuk, P. V. et al. Excitation of ^{229}Th nuclei in laser plasma: the energy and half-life of the low-lying isomeric state. Preprint at <https://arxiv.org/abs/1804.00299> (2018).
62. Stellmer, S., Schreitl, M. & Schumm, T. Radioluminescence and photoluminescence of Th:CaF_2 crystals. *Sci. Rep.* **5**, 15580 (2015).
63. Reich, C. W., Helmer, R. G., Baker, J. D. & Gehrke, R. J. Emission probabilities and energies of γ -ray transitions from the decay of ^{233}U . *Int. J. Appl. Radiat. Isot.* **35**, 185–188 (1984).
64. Reich, C. W. & Helmer, R. G. Energy separation of the doublet of intrinsic states at the ground state of ^{229}Th . *Phys. Rev. Lett.* **64**, 271–273 (1990).
65. Helmer, R. G. & Reich, C. W. An excited state of ^{229}Th at 3.5 eV. *Phys. Rev. C* **49**, 1845–1858 (1994).
66. Irwin, G. M. & Kim, K. H. Observation of electromagnetic radiation from deexcitation of the ^{229}Th isomer. *Phys. Rev. Lett.* **79**, 990–993 (1997).
67. Richardson, D. S., Benton, D. M., Evans, D. E., Griffith, J. A. R. & Tongate, G. Ultraviolet photon emission observed in the search for the decay of the ^{229}Th isomer. *Phys. Rev. Lett.* **80**, 3206–3208 (1998).
68. Shaw, R. W., Young, J. P., Cooper, S. P. & Webb, O. F. Spontaneous ultraviolet emission from ^{235}U / ^{229}Th samples. *Phys. Rev. Lett.* **82**, 1109–1111 (1999).
69. Utter, S. B. et al. Reexamination of the optical gamma ray decay in ^{229}Th . *Phys. Rev. Lett.* **82**, 505–508 (1999).
70. Guimaraes-Filho, Z. O. & Helene, O. Energy of the 3/2⁺ state of ^{229}Th reexamined. *Phys. Rev. C* **71**, 044303 (2005).
71. Beck, B. R. et al. *Improved Value for the Energy Splitting of the Ground-state Doublet in the Nucleus ^{229}Th* . Report No. LLNL-PROC-415170 (Lawrence Livermore National Lab, 2009).
72. Kazakov, G. A., Schumm, T. & Stellmer, S. Re-evaluation of the Beck et al. data to constrain the energy of the Th-229 isomer. Preprint at <https://arxiv.org/abs/1702.00749> (2017).
73. Sikorsky, T. et al. Measurement of the ^{229}Th isomer energy with a magnetic micro-calorimeter. *Phys. Rev. Lett.* **125**, 142503 (2020). **Currently the most precise γ -spectroscopic measurement of the isomer energy.**
74. von der Wense, L. et al. Direct detection of the ^{229}Th nuclear clock transition. *Nature* **533**, 47–51 (2016). **Direct detection of the isomer in recoil ions from the decay of ^{233}U .**
75. Church, E. L. & Wenner, J. Nuclear structure effects in internal conversion. *Annu. Rev. Nucl. Sci.* **10**, 193–234 (1960).
76. Seiferle, B. et al. Energy of the ^{229}Th nuclear clock transition. *Nature* **573**, 243–246 (2019). **Currently the most precise conversion electron measurement of the isomer energy.**
77. von der Wense, L. & Zhang, C. Concepts for direct frequency-comb spectroscopy of ^{229}Th and an internal-conversion-based solid-state nuclear clock. *Eur. Phys. J. D* **74**, 146 (2020).
78. Seiferle, B. *Characterization of the ^{229}Th Nuclear Clock Transition*. PhD thesis, Ludwig-Maximilians Univ. (2019).
79. Gerstenkorn, S. et al. Structures hyperfinies du spectre d'étalement, moment magnétique et quadrupolaire de l'isotope 229 du thorium. *J. Phys.* **35**, 483–495 (1974).
80. Bemis, C. E. et al. Coulomb excitation of states in ^{229}Th . *Phys. Scr.* **38**, 657–663 (1988).
81. Tkalya, E. V. Proposal for a nuclear gamma-ray laser of optical range. *Phys. Rev. Lett.* **106**, 162501 (2011).
82. Dykhne, A. M. & Tkalya, E. V. Matrix element of the anomalously low-energy (3.5 ± 0.5 eV) transition in ^{229}Th and the isomer lifetime. *JETP Lett.* **67**, 251–256 (1998).
83. Minkov, N. & Pálffy, A. Theoretical predictions for the magnetic dipole moment of ^{229}Th . *Phys. Rev. Lett.* **122**, 162502 (2019).
84. Hayes, A. C., Friar, J. L. & Möller, P. Splitting sensitivity of the ground and 7.6-eV isomeric states of ^{229}Th . *Phys. Rev. C* **78**, 024311 (2008).
85. Berengut, J. C., Dzuba, V. A., Flambaum, V. V. & Porsev, S. G. Proposed experimental method to determine a sensitivity of splitting between ground and 7.6-eV isomeric states in ^{229}Th . *Phys. Rev. Lett.* **102**, 210801 (2009).
86. Porsev, S. G. & Flambaum, V. V. Electronic bridge process in ^{229}Th . *Phys. Rev. A* **81**, 042516 (2010).
87. Karpechin, F. F., Band, I. M. & Trzhaskovskaya, M. B. 3.5-eV isomer of ^{229}Th : how it can be produced. *Nucl. Phys. A* **654**, 579–596 (1999).
88. Krutov, V. A. & Fomenko, V. N. Influence of electronic shell on gamma radiation of atomic nuclei. *Ann. Phys.* **476**, 291–302 (1968).
89. Morita, M. Nuclear excitation by electron transition and its application to uranium 235 separation. *Prog. Theor. Phys.* **49**, 1574–1586 (1973).
90. Izawa, Y. & Yamanaka, C. Production of ^{235}U by nuclear excitation by electron transition in a laser produced uranium plasma. *Phys. Lett.* **B 88**, 59–61 (1979).
91. Strizhov, V. & Tkalya, E. Decay channel of low-lying isomer state of the ^{229}Th nucleus. *Sov. Phys. JETP* **72**, 387–390 (1991).
92. Herrera-Sancho, O. A., Nemitz, N., Okhaphin, M. V. & Peik, E. Energy levels of Th^+ between 7.3 and 8.3 eV. *Phys. Rev. A* **88**, 1–7 (2013).
93. Porsev, S. G., Flambaum, V. V., Peik, E. & Tamm, C. Excitation of the isomeric ^{229}Th nuclear state via an electronic bridge process in ^{229}Th . *Phys. Rev. Lett.* **105**, 182501 (2010).
94. Müller, R. A., Volotka, A. V. & Surzhykov, A. Excitation of the ^{229}Th nucleus via a two-photon electronic transition. *Phys. Rev. A* **99**, 042517 (2019).
95. Meier, D. M. *Electronic level structure investigations in Th^+ in the energy range of the ^{229}Th isomer*. PhD thesis, Leibniz Univ. (2019).
96. Thielking, J. *Hyperfine Studies of Th-229 in its Nuclear Ground and Isomeric State*. PhD thesis, Leibniz Univ. (2020).
97. Bilous, P. V. et al. Electronic bridge excitation in highly charged ^{229}Th ions. *Phys. Rev. Lett.* **124**, 192502 (2020).
98. Bilous, P. V., Minkov, N. & Pálffy, A. Electric quadrupole channel of the 7.8-eV ^{229}Th transition. *Phys. Rev. C* **97**, 044320 (2018).
99. Yamaguchi, A. et al. Experimental search for the low-energy nuclear transition in ^{229}Th with undulator radiation. *N. J. Phys.* **17**, 053053 (2015).
100. Kang, L., Lin, Z., Liu, F. & Huang, B. Removal of A-site alkali and alkaline earth metal cations in $\text{KBe}_2\text{BO}_3\text{F}_2$ -type layered structures to enhance the deep-ultraviolet nonlinear optical capability. *Inorg. Chem.* **57**, 11146–11156 (2018).
101. Kanai, T. et al. Generation of vacuum-ultraviolet light below 160 nm in a KBBF crystal by the fifth harmonic of a single-mode Ti:sapphire laser. *J. Opt. Soc. Am. B* **21**, 370 (2004).
102. Nakazato, T. et al. Phase-matched frequency conversion below 150 nm in $\text{KBe}_2\text{BO}_3\text{F}_2$. *Opt. Express* **24**, 17149 (2016).
103. Bjorklund, G. C. Effects of focusing on third-order nonlinear processes in isotropic media. *IEEE J. Quantum Electron.* **11**, 287–296 (1975).
104. Hilbig, R., Hilber, G., Lago, A., Wolff, B. & Wallenstein, R. Tunable coherent VUV radiation generated by nonlinear optical frequency conversion in gases. *Proc. SPIE* **0613**, <https://doi.org/10.1117/12.960383> (1986).
105. Hanna, S. J. et al. A new broadly tunable (7.4–10.2 eV) laser based VUV light source and its first application to aerosol mass spectrometry. *Int. J. Mass. Spectrom.* **279**, 134–146 (2009).
106. Gohle, C. et al. A frequency comb in the extreme ultraviolet. *Nature* **436**, 234–237 (2005).
107. Jones, R. J., Moll, K. D., Thorpe, M. J. & Ye, J. Phase-coherent frequency combs in the vacuum ultraviolet via high-harmonic generation inside a femtosecond enhancement cavity. *Phys. Rev. Lett.* **94**, 193201 (2005).
108. Witte, S., Zinkstok, R. T., Ubachs, W., Hogervorst, W. & Eikema, K. S. E. Deep-ultraviolet quantum interference metrology with ultrashort laser pulses. *Science* **307**, 400–403 (2005).

109. Yost, D. C. et al. Vacuum-ultraviolet frequency combs from below-threshold harmonics. *Nat. Phys.* **5**, 815–820 (2009).
110. Seres, J. et al. All-solid-state VUV frequency comb at 160 nm using high-harmonic generation in nonlinear femtosecond enhancement cavity. *Opt. Express* **27**, 6618–6628 (2019).
111. Cingöz, A. et al. Direct frequency comb spectroscopy in the extreme ultraviolet. *Nature* **482**, 68–71 (2012).
112. Ozawa, A. & Kobayashi, Y. VUV frequency-comb spectroscopy of atomic xenon. *Phys. Rev. A* **87**, 022507 (2013).
113. Hilborn, R. C. Einstein coefficients, cross sections, f values, dipole moments, and all that. *Am. J. Phys.* **50**, 982–986 (1982).
114. Cohen-Tannoudji, C. & Guéry-Odelin, D. *Advances in Atomic Physics: An Overview* (World Scientific, 2011).
115. Safronova, M. S. et al. Search for new physics with atoms and molecules. *Rev. Mod. Phys.* **90**, 025008 (2018).
116. Fadeev, P., Berengut, J. C. & Flambaum, V. V. Sensitivity of ^{229}Th nuclear clock transition to variation of the fine-structure constant. *Phys. Rev. A* **102**, 052833 (2020).
117. Flambaum, V. V. Enhanced effect of temporal variation of the fine structure constant and the strong interaction in ^{229}Th . *Phys. Rev. Lett.* **97**, 092502 (2006). **Prediction of the unusually high sensitivity of a ^{229}Th clock in a search for variations of fundamental constants.**
118. Flambaum, V. V. & Wiringa, R. B. Enhanced effect of quark mass variation in ^{229}Th and limits from Oklo data. *Phys. Rev. C* **79**, 034301 (2009).
119. Stadnik, Y. V. & Flambaum, V. V. Can dark matter induce cosmological evolution of the fundamental constants of nature? *Phys. Rev. Lett.* **115**, 201301 (2015).
120. Flambaum, V. V. Enhancing the effect of Lorentz invariance and Einstein's equivalence principle violation in nuclei and atoms. *Phys. Rev. Lett.* **117**, 072501 (2016).
121. Magnetic micro-calorimeter raw data. <https://zenodo.org/record/3931904#.X5WqQYj7SUI> [Zenodo, 2020].

Acknowledgements

Our work on ^{229}Th was supported by the European Union's Horizon 2020 research and innovation programme under

grant agreement no. 664732 "nuClock", grant agreement no. 856415 "ThoriumNuclearClock" and grant agreement no. 882708 "CrystalClock". The team has also received funding from the EMPIR project "CC4C". This project has received funding from the EMPIR programme co-financed by the Participating States and from the European Union's Horizon 2020 research and innovation programme.

Author contributions

The authors contributed equally to all aspects of the article.

Competing interests

The authors declare no competing interests.

Peer review information

Nature Reviews Physics thanks Victor Flambaum, David Leibrandt and the other, anonymous, reviewer for their contribution to the peer review of this work.

Publisher's note

Springer Nature remains neutral with regard to jurisdictional claims in published maps and institutional affiliations.

© Springer Nature Limited 2021